Cervelleite, Ag4TeS: solution and description of the crystal structure

Mineralogy and Petrology

Cervelleite, Ag4TeS: solution and description of the crystal structure

--Manuscript Draft--

Manuscript Number:	MIPE-D-15-00008R1
Full Title:	Cervelleite, Ag4TeS: solution and description of the crystal structure
Article Type:	Standard Article
Keywords:	cervelleite; Ag-Te-S system; Ag-Cu sulfotellurides; crystal structure; aguilarite; acanthite
Corresponding Author:	Luca Bindi, Prof University of Florence Florence, ITALY
Corresponding Author Secondary Information:	
Corresponding Author's Institution:	University of Florence
Corresponding Author's Secondary Institution:	
First Author:	Luca Bindi, Prof
First Author Secondary Information:	
Order of Authors:	Luca Bindi, Prof
	Christopher Stanley
	Paul G Spry
Order of Authors Secondary Information:	
Funding Information:	
Abstract:	Examination of the type specimen of cervelleite throws new light on its structure demonstrating how earlier researchers erred in describing the mineral as cubic. It was found to be monoclinic, space group P21/n, with a = 4.2696(4), b = 6.9761(5), c = 8.0423(7) Å, β = 100.332(6)°, V = 235.66(3) Å3, Z = 4. The crystal structure [R1 = 0.0329 for 956 reflections with I > 2σ(I)] is topologically identical to that of acanthite, Ag2S, and aguilarite, Ag4SeS. It can be described as a body-centered array of tetrahedrally coordinated X atoms (where X = S and Te) with Ag2X4 polyhedra in planes nearly parallel to (010); the sheets are linked by the other silver position (i.e., Ag1) that exhibits a three-fold coordination. Crystal-chemical features are discussed in relation to other copper and silver sulfides/tellurides, and pure metals. A SEM study of the cervelleite crystal used for the structural investigation showed that it is intergrown with an unnamed Ag2FeS2 phase in the type material.
Response to Reviewers:	Dear Anton, Please find herewith the revised copy of the manuscript entitled “Cervelleite, Ag4TeS: solution and description of the crystal structure” by Luca Bindi, Christopher J. Stanley, and Paul G. Spry. We did the minor stylistic changes suggested by the reviewers. We think that it is not necessary to add the Table as suggested by Rev#2. With best regards, Luca Bindi

Cervelleite, Ag_4TeS: solution and description of the crystal structure

L. Bindi [a] · **C.J. Stanley** [b] · **P.G. Spry** [c]

[a] Dipartimento di Scienze della Terra, Università di Firenze, Via G. La Pira 4, I-50121Firenze, Italy

[b] Department of Earth Sciences, Natural History Museum, Cromwell Road, London SW7 5BD, United Kingdom

[c] Department of Geological and Atmospheric Sciences, 253 Science I, Iowa State University, Ames, Iowa 50011-3212, U.S.A.

Corresponding author:

Luca Bindi
Dipartimento di Scienze della Terra,
Università di Firenze
Via G. La Pira 4, I-50121 Firenze, Italy
Tel. +39-055-2757532
Fax +39-055-2757455
e-mail: luca.bindi@unifi.it

Keywords: cervelleite · Ag-Te-S system · Ag-Cu sulfotellurides · crystal structure · aguilarite · acanthite

Abstract

Examination of the type specimen of cervelleite throws new light on its structure demonstrating how earlier researchers erred in describing the mineral as cubic. It was found to be monoclinic, space group $P2_1/n$, with a = 4.2696(4), b = 6.9761(5), c = 8.0423(7) Å, β = 100.332(6)°, V = 235.66(3) Å^3, Z = 4. The crystal structure [$R1$ = 0.0329 for 956 reflections with $I > 2\sigma(I)$] is topologically identical to that of acanthite, Ag_2S, and aguilarite, Ag_4SeS. It can be described as a body-centered array of tetrahedrally coordinated X atoms (where X = S and Te) with $Ag2X_4$ polyhedra in planes nearly parallel to (010); the sheets are linked by the other silver position (i.e., Ag1) that exhibits a three-fold coordination. Crystal-chemical features are discussed in relation to other copper and silver sulfides/tellurides, and pure metals. A SEM study of the cervelleite crystal used for the structural investigation showed that it is intergrown with an unnamed Ag_2FeS_2 phase in the type material.

Introduction

Silver chalcogenides have received much attention in recent years because of their important technological applications (e.g., Padma Kumar and Yashonath 2006). These compounds are known to be fast ionic conductors or semiconductors and, as such, find practical applications in silver photography as sensitizers or in optics and microelectronics as rewritable storage media. From a geological standpoint, silver sulfotellurides are trace constituents accompanying native gold and Au-Ag-tellurides in various deposit types that span the magmatic-hydrothermal spectrum.

In the system Ag-Te-S, cervelleite Ag_4TeS is of particular interest because it occurs as an accessory mineral in a range of hydrothermal precious mineral deposits (Cook and Ciobanu 2003). It was defined as a new mineral species by Criddle et al.

(1989) during a study of ore minerals collected from the spoil tips of the abandoned Bambolla mine, Moctezuma, Sonora (Mexico). By means of X-ray photographic techniques, these authors studied fragments of cervelleite intergrown with acanthite from a structural point of view and reported a cubic symmetry (with *P*23*, Pm*3*, P*432*, P*43*m*, *Pm*3*m, P*2_13*,* P4_232, *P*4_132*,* P4_332*, Pa*3 as possible space groups) with *a* = 14.03(1) and *Z* = 24. Criddle et al. (1989) also noticed that cervelleite, acanthite and hessite were altered rapidly and profoundly by light, in a surface reaction interpreted as photo-chemical in origin.

Cervelleite, along with other cervelleite-like minerals, has been reported from various ore types including the intrusion-hosted San Martin deposit, Argentina (Paar and De Brodtkorb 1996), the epithermal Mayflower Au-Ag deposit, Montana (Spry and Thieben 1996), the Um Samiuki volcanogeneic massive sulfide deposit, Egypt (Helmy 1999), epithermal (Larga, Roşia Montană) and skarn (Băița Bihor and Ocna de Fier) occurrences in Romania (Cook and Ciobanu 2003; Ciobanu et al. 2004), the Eniovche epithermal deposit, Bulgaria (Dobrev et al. 2002), the intrusion-hosted Funan Au deposit, China (Gu et al. 2003), and several volcanic-hosted massive sulfide deposits in the southern Urals (Novoselov et al. 2006). Unnamed Ag-sulfotellurides [$(Ag,Cu)_6TeS_2$ – $(Ag,Cu)_4TeS$] were described from the Funan deposit (Gu et al. 2003), and a phase with the composition Ag_2Cu_2TeS was reported by Cook and Ciobanu (2003) from the Băița Bihor and Ocna de Fier skarns in Romania. In Greece, cuprian cervelleite and unnamed Ag-Cu sulfotellurides [$(Ag,Cu)_{12}Te_3S_2$ and $(Ag,Au,Cu)_9Te_2S_3$] were described from the intrusion-related deposit at Panormos Bay, Tinos Island (Tombros et al. 2004, 2010; Spry et al. 2006). In the Kallianou area (southern Evia Island, Greece), gold-bearing quartz veins contain an exotic ore mineralogy including cervelleite-like sulfotellurides [Ag_2CuTeS and $(Ag,Cu)_2Te$] and

Te-rich polybasite (Voudouris and Spry 2008; Voudouris et al. 2011; Bindi et al. 2013b).

In the course of a research project dealing with the description and structural characterization of natural copper and silver tellurides (Bindi 2008, 2009, 2014; Bindi and Cipriani 2004; Bindi and Pinch 2014; Bindi and Pingitore 2013; Bindi et al. 2004, 2005, 2009, 2013a, 2013b), we have examined a fragment of cervelleite from the holotype material (catalogue number E.1161 BM 1985, 354).

The holotype

The specimen was collected by the late Alan Criddle on a field excursion to the Sonora Desert led by the late Sid Williams. It consists of black powdery crusts (1–2 mm thick) of benleonardite, acanthite, hessite and cervelleite, together with gangue quartz and dolomite (Fig. 1). The hessite contains a vermiform or myrmekitic intergrowth of fine-grained cervelleite (pale-greenish-grey in Fig. 1). The assemblage occupies irregular fractures in a highly altered rock described by Williams (1982) as an intensely silicified rhyolitic vitrophyre.

Crystal-structure solution and refinement

A small crystal fragment (40 × 55 × 60 μm) was selected from the type specimen for the X-ray single-crystal diffraction study that was done with an Oxford Diffraction Xcalibur 3 CCD single-crystal diffractometer (Table 1). Surprisingly, most of the X-ray reflections (89% of the total) match the following monoclinic unit cell: a ~ 4.30, b ~ 6.98, c ~ 8.04 Å and β ~ 100°, being very close to those of acanthite, Ag_2S (Frueh 1958) and aguilarite (Bindi and Pingitore 2013). The other 11% of the total reflections could be indexed according to the following monoclinic (primitive) unit cell:

a ~ 9.00, *b* ~ 12.56, *c* ~ 5.76 Å, β = 94° (*vide infra*). The data were reduced taking into account the first monoclinic cell. Systematic absences (*h*0*l*: *h* + *l* = 2n; *h*00: *h* = 2n; 0*k*0: *k* = 2n; 00*l*: *l* = 2n) were consistent with the space groups $P2_1/n$ ($P2_1/c$ as standard). Statistical tests on the distribution of |*E*| values strongly indicate the presence of an inversion centre ($|E^2-1|$ = 0.922), thus supporting the choice of the space group $P2_1/n$. We decided to refine the cervelleite structure in the non-standard space group $P2_1/n$ in order to have the same orientation reported for acanthite and aguilarite. The program SHELXL (Sheldrick 2008) was used for the refinement of the structure, which was carried out starting from the atomic coordinates of acanthite by Frueh (1958). The occupancy of all the sites was left free to vary (Ag vs. vacancy; Te vs. S) and then fixed to the resulting value. The refined values are given in Table 2. Neutral scattering curves for Ag, S and Te were taken from the *International Tables for X-ray Crystallography* (Ibers and Hamilton 1974). At the last stage, with anisotropic atomic displacement parameters for all atoms and no constraints, the residual value settled at *R* = 0.0298 for 418 observed reflections [2σ(*I*) level] and 29 parameters and at *R* = 0.0329 for all 956 independent reflections. Experimental details and *R* indices are given in Table 1. Fractional atomic coordinates and isotropic displacement parameters are reported in Table 2 (anisotropic ADPs can be found in the accompanying CIF). Bond distances are given in Table 3. The calculated X-ray powder-diffraction pattern, computed with the atom coordinates and occupancies reported in Table 2, is given in Table 4. Structure factors and CIF are available from the authors upon request.

Results and Discussion

Description of the crystal structure

The crystal structure of cervelleite (Fig. 2) is topologically identical to that of acanthite (Frueh 1958) and aguilarite (Bindi and Pingitore 2013). It can be described as a body-centered array of tetrahedrally coordinated X atoms (where X = S, Se and Te) with Ag2-polyhedra in planes nearly parallel to (010); the sheets are linked by the other silver position (i.e., Ag1) that exhibits a three-fold coordination. Due to the greater size of Te compared to S and Se, Ag1 and Ag2 atoms in cervelleite increase their coordination number to 3 and 4, respectively, with respect to that observed in acanthite and aguilarite (2 and 3 for Ag1 and Ag2, respectively). Results indicate that Z = 4 [with an unit-cell volume of 235.66(3) Å^3 and formula $Ag_2(Te_{0.50}S_{0.50})$], unlike the findings of Criddle et al. (1989) that reported Z = 24 [with unit-cell volume of 2762(2) Å^3 and formula Ag_4TeS]. As such, the computed density should be 8.247 g/cm^3 rather than the value of 8.53 g/cm^3 reported previously.

In the structure, the bond distances observed for the two silver positions (i.e., <Ag1–X> = 2.660 Å and <Ag2–X> = 2.729 Å) are larger than those observed in acanthite [<Ag1–X> = 2.503 Å and <Ag2–X> = 2.602 Å, Frueh (1958)] and aguilarite [<Ag1–X> = 2.511 Å and <Ag2–X> = 2.628 Å, Bindi and Pingitore (2013)], due to the greater size of Te compared to Se and S (Shannon 1976). On the whole, the observed Ag–X bond distances (Table 3) are intermediate with respect to the Ag–Te distances observed in hessite, Ag_2Te (2.84–3.03 Å; Van der Lee and de Boer 1993), sylvanite, $(Au,Ag)_2Te_4$ (2.74–3.23 Å; Pertlik 1984), muthmannite, $AuAgTe_2$ (2.69–2.97 Å; Bindi and Cipriani 2004), and empressite, AgTe (2.84–2.96 Å; Bindi et al. 2004), and those observed for some Ag–Se minerals (e.g., naumannite, Ag_2Se, 2.62–2.86 Å, Wiegers 1971; aguilarite, Ag_4SeS, 2.51–2.63 Å, Bindi and Pingitore 2013).

The shortest Ag–Ag contact in cervelleite (Ag2–Ag2 = 2.968 Å) is nearly identical to the corresponding value in naumannite (Ag–Ag = 2.93 Å, Wiegers 1971), and is very similar to those observed in *fcc* silver (Ag–Ag = 2.89 Å; Suh et al. 1988) or *hcp* silver [Ag–Ag = 2.93 Å; Petruk et al. 1970]. The mean electron number refined for the X position [0.527(3)Te + 0.473S = 34.97] is in excellent agreement with the chemical formula reported in the literature for cervelleite, i.e. Ag_4TeS.

In Figure 3, the unit-cell volumes of synthetic members belonging to the two solid solutions, the monoclinic 'acanthite-like' Ag_2S – $Ag_2S_{0.4}Se_{0.6}$ series and the orthorhombic 'naumannite-like' $Ag_2S_{0.3}Se_{0.7}$ – Ag_2Se series (Pingitore et al. 1992), are plotted against the selenium contents. A good linear trend is observed corresponding to the expansion of the lattice dimensions as the larger Se^{2-} anion replaces S^{2-}, following Vegard's law for the properties of solid solutions. Taking into consideration the ionic radii of Te, Se and S, if we calculate a mean value for cervelleite ($Te_{0.50}S_{0.50}$) and then extrapolate the potential amount of Se (to plot it in Figure 3), we can see that the studied crystal (filled circle) occurs along this trend.

Discussion of the previous results obtained by Criddle et al. (1989)

We have here unambiguously shown for the first time that cervelleite represents the Te-analogue of aguilarite. However, a puzzling aspect of the current study is that Criddle et al. (1989) described cervelleite as an optically isotropic mineral with a cubic symmetry. We note here that the same set of *d* spacings reported by Criddle et al. (1989), which are indexed with a primitive cubic lattice with *a* = 14.03 Å, can be obtained with the monoclinic unit cell found in this study and matching the 11% of the total reflections collected from our 'cervelleite' crystal. The refined monoclinic unit cell can be written as *a* = 8.994(8), *b* = 12.56(1), *c* = 5.761(6) Å, β = 93.90(8)°, *V* =

649.3(9) Å^3 and the comparison with the diffraction pattern originally reported by Criddle et al. (1989) is given in Table 5.

We surmise that Criddle et al. (1989) obtained chemical and optical data on cervelleite but carried out X-ray data on this second monoclinic unknown phase. This unknown phase is intergrown with cervelleite, and occurs in variable amounts. To corroborate these findings, we embedded the cervelleite grain in epoxy used for the structural investigation and studied the polished section by means of a scanning electron microscope. The grain appears to be formed of two phases (Fig. 4): a brighter phase which shows the composition typically observed for cervelleite (i.e., Ag_4TeS, when the data are normalized on the basis of 6 atoms per formula unit), and a darker phase with stoichiometry Ag_2FeS_2, which is likely responsible for the diffraction peaks belonging to the second monoclinic unit cell [i.e., *a* = 8.994(8), *b* = 12.56(1), *c* = 5.761(6) Å, β = 93.90(8)°]. Unfortunately, the very low number of reflections for this unnamed Ag_2FeS_2 phase precludes any *ab initio* structure determination. The search for grains composed of this potential new mineral only failed.

Thus, the holotype sample contains cervelleite, benleonardite and an unknown (likely) new Ag-Fe-S phase exhibiting the second monoclinic unit-cell identified here (which replaced the cubic cell given by Criddle et al. 1989).

Conclusions

1. Cervelleite is monoclinic, space group $P2_1/n$, with *a* = 4.2696(4), *b* = 6.9761(5), *c* = 8.0423(7) Å, β = 100.332(6)°, *V* = 235.66(3) Å^3, Z = 4. The crystal structure [*R*1 = 0.0329 for 956 reflections with $I > 2\sigma(I)$], solved for the first time, demonstrates that the mineral is the Te-analogue of aguilarite.

2. Cervelleite coexists with an unnamed Ag_2FeS_2 phase in the type sample. The unnamed phase exhibits a monoclinic symmetry with cell dimensions: *a* = 8.994(8), *b* = 12.56(1), *c* = 5.761(6) Å, β = 93.90(8)° and *V* = 649.3(9) $Å^3$. The comparison with the diffraction pattern originally reported by Criddle et al. (1989) gave an excellent match.
3. The museum specimen studied here (catalogue number E.1161 BM 1985, 354) is the type sample for cervelleite, benleonardite and a new previously unidentified Ag-Fe-S phase.

Acknowledgements Mike Rumsey is thanked for providing us with the holotype sample of cervelleite. The paper benefited by the official reviews made by Panagiotis Voudouris and an anonymous reviewer. Associate Editor Anton Beran is thanked for his efficient handling of the manuscript. This work was supported by “Progetto d’Ateneo 2012, University of Firenze” to LB.

References

Bindi L (2008) Commensurate-incommensurate phase transition in muthmannite, $AuAgTe_2$: First evidence of a modulated structure at low-temperature. Phil Mag Lett 88:533–541

Bindi L (2009) Thermal expansion behavior of empressite, AgTe: A structural study by means of in situ high-temperature single-crystal X-ray diffraction. J Alloys Comp 473:262–264

Bindi L (2014) Chemical and structural characterization of henryite, $(Cu,Ag)_{3+x}Te_2$ (x ~ 0.40): A new structure type in the (Ag)-Cu-Te system. Solid State Sci 38:108–111

Bindi L, Arakcheeva A, Chapuis G (2009) The role of silver on the stabilization of the incommensurately modulated structure in calaverite, $AuTe_2$. Am Mineral 94:728–736.

Bindi L, Carbone C, Belmonte D, Cabella R, Bracco R (2013a) Weissite from Gambatesa mine, Val Graveglia, Liguria, Italy: occurrence, composition and determination of the crystal structure. Mineral Mag 77:475–483

Bindi L, Cipriani C (2004) Ordered distribution of Au and Ag in the crystal structure of muthmannite, $AuAgTe_2$, a rare telluride from Sacarîmb, western Romania. Am Mineral 89:1505–1509

Bindi L, Pinch WW (2014) Cameronite, $Cu_{5-x}(Cu,Ag)_{3+x}Te_{10}$ (x = 0.43), from the Good Hope Mine, Vulcan, Colorado: Crystal structure and revision of the chemical formula. Can Mineral 52:423–432

Bindi L, Pingitore NE (2013) On the symmetry and crystal structure of aguilarite, Ag_4SeS. Mineral Mag 77:21–31

Bindi L, Rossell Abrodos M, Van Tendeloo G, Spry PG, Cipriani C (2005) Inferred phase relations in part of the system Au-Ag-Te: an integrated analytical study of gold ore from the Golden Mile, Kalgoorlie, Australia. Mineral Petrol 83:283–293

Bindi L, Spry PG, Cipriani C (2004) Empressite, AgTe, from the Empress-Josephine Mine, Colorado, USA: composition, physical properties and determination of the crystal structure. Am Mineral 89:1043–1047

Bindi L, Voudouris P, Spry PG (2013b) Structural role of tellurium in the minerals of the pearceite-polybasite group. Mineral Mag 77:419–428

Ciobanu CL, Cook NJ, Tămaş C, Leary S, Manske S, O'Connor G, Minuț A (2004) Tellurides-gold-base metal associations at Roşia Montană: the role of hessite as gold carrier. In: Cook N, Ciobanu CL (eds) Au-Ag-telluride deposits of the Golden Quadrilateral, Apuseni Mts., Romania, IAGOD Guidebook Ser 12, 187–202

Cook NJ, Ciobanu CL (2003) Cervelleite, Ag_4TeS, from three, localities in Romania, substitution of Cu, and the occurrence of the associated phase, Ag_2Cu_2TeS. N Jb Miner Mh 7:321–336

Criddle AJ, Chisholm JE, Stanley CJ (1989) Cervelleite, Ag_4TeS, a new mineral from the Bambolla mine, Mexico, and a description of a photo-chemical reaction involving cervelleite, acanthite and hessite. Eur J Miner 1:371–380

Dobrev S, Strashimirov S, Vassileva M, Dragiev H (2002) Silver and silver-bearing phases from Chala and Pcheloiad deposits (Eastern Rhodopes) and Eniovche deposit (Central Rhodopes). Univ Mining and Geology "St. Ivan Rilski" Annual: 1–6

Downs RT, Bartelmehs KL, Gibbs GV, Boisen MBJr (1993) Interactive software for calculating and displaying X-ray or neutron powder diffractometer patterns of crystalline materials. Am Mineral 78:1104–1107

Frueh AJ Jr (1958) The crystallography of silver sulfide, Ag_2S. Zeit Kristallogr 110:136–144

Gu XP, Watanabe M, Hoshino K, Shibata Y (2003) New find of silver tellurosulphides from the Funan gold deposit, East Shandong, China. Eur J Miner 15:147–155

Helmy HM (1999) The Um Samiuki volcanogenic Zn-Cu-Pb-Ag deposit, Eastern Desert, Egypt: a possible new occurrence of cervelleite. Can Miner 37:143–158

Ibers JA, Hamilton WC Eds (1974) *International Tables for X-ray Crystallography*, vol. IV, 366p. Kynock, Dordrecht, The Netherlands

Novoselov KA, Belogub EV, Zykov VV, Yakovleva VA (2006) Silver sulfotellurides from volcanic-hosted massive sulphide deposits in the Southern Urals. Mineral Petrol 87:327–349

Oxford Diffraction (2006) *CrysAlis* RED (Version 1.171.31.2) and ABSPACK in *CrysAlis* RED. Oxford Diffraction Ltd, Abingdon, Oxfordshire, England

Paar W, De Brodtkorb MK (1996) Presencia de cervelleíta y hessita en la galena del yacimiento San Martín, Valcheta, prov. de Río Negro. 3° Reunión de Mineralogía y Metalogenia, Instituto de Recursos Minerales. Univ. Nacional de La Plata, Argentina Publ. No. 5: 173–175

Padma Kumar P, Yashonath S (2006) Ionic conduction in the solid state. J Chem Sci 118:135–154

Pertlik F (1984) Kristallchemie natürlicher Telluride I: Verfeinerung der Kristallstruktur des Sylvanits, $AuAgTe_4$. Tsch Mineral Petrograph Mitt 33:203–212

Petruk W, Cabri LJ, Harris DC, Stewart JM, Clark LA (1970) Allargentum, redefined. Can Mineral 10:163–172

Pingitore NE, Ponce BF, Moreno F, Podpora C (1992) Solid solutions in the system Ag_2S–Ag_2Se. J Mat Res 7:2219–2224

Shannon RD (1976) Revised effective ionic radii and systematic studies of interatomic distances in halides and chalcogenides. Acta Crystallogr A32:751–767

Sheldrick GM (2008) A short history of SHELX. Acta Crystallogr A64:112–122

Suh I-K, Ohta H, Waseda Y (1988) High-temperature thermal expansion of six metallic elements measured by dilatation method and X-ray diffraction. J Mat Sci 23:757–760.

Spry PG, Thieben SE (1996) Two new occurrences of benleonardite, a rare silver tellurium sulphosalt, and a possible new occurrence of cervelleite. Miner Mag 60:871–876

Spry PG, Tombros SF, Seymour KSt, Williams-Jones AE, Zouzias DP (2006) Geology, mineralogy and geochemistry of granite-hosted gold telluride mineralization at Panormos Bay, Tinos Island, Greece. Geol Soc Am Abstr 38:55

Tombros S, Seymour KSt, Spry PG (2004) Description and conditions of formation of new unnamed Ag-Cu and Ag-Cu-Au sulfotellurides in epithermal polymetallic Ag-Au-Te mineralization, Tinos Island, Hellas. N Jb Miner Abh 179:295–310

Tombros SF, Seymour KSt, Williams-Jones AE (2010) Controls on tellurium in base, precious, and telluride minerals in the Panormos Bay Ag-Au-Te deposits, Tinos Island, Cyclades, Greece. Econ Geol 105:1097–1111

Van der Lee A, de Boer JL (1993) Redetermination of the structure of hessite, Ag_2Te-III. Acta Crystallogr C49:1444–1446

Voudouris P, Spry PG (2008) A new occurrence of cervelleite-like phases and Te-polybasite from gold-bearing veins in metamorphic rocks of the Cycladic Blueschist Unit, Greece. 33rd International Geological Congress, MRD-09 Au-Ag tellurideselenide deposits, CD-ROM, Abstract

Voudouris P, Spry PG, Sakellaris GA, Mavrogonatos C (2011) A cervelleite-like mineral and other Ag-Cu-Te-S minerals [Ag_2CuTeS and $(Ag,Cu)_2TeS$] in gold-bearing veins in metamorphic rocks of the Cycladic Blueschist Unit, Kallianou, Evia Island, Greece. Miner Petrol 101:169–183

Wiegers GA (1971) The crystal structure of the low-temperature form of silver selenide. Am Mineral 56:1882–1888

Williams SA (1982) Cuzticite and eztlite, two new tellurium minerals from Moctezuma, Mexico. Mineral Mag 46:257–259

Figure Captions

Figure 1 – Reflected plane polarized light digital image (in oil immersion) illustrating pale greenish cervelleite overgrowths on acanthite rosettes (with intergrown unknown phase) and coarser acanthite (near scale bar) and quartz (middle left). Creamy white hessite forms the infill. The sample (catalogue number E.1161 BM 1985, 354) is the type specimen for both cervelleite and benleonardite.

Figure 2 – The crystal structure of cervelleite projected down [100]. The horizontal direction is the *c* axis. Ag and X (S and Te) are given as white and black spheres, respectively. The unit cell is outlined.

Figure 3 – The unit-cell volume ($Å^3$) plotted against the Se content (a.p.f.u.). Filled symbol represents the cervelleite crystal (this study), whereas empty symbols are data from synthetic compounds (Pingitore et al. 1992).

Figure 4 – SEM-BSE image showing the coexistence of two phases (brighter: cervelleite, darker: unnamed Ag_2FeS_2) in the crystal used for the structural investigation.

Table
Click here to download Table: Bindi et al_Table 1.doc

TABLE 1 – Crystallographic data and refinement parameters for cervelleite

Crystal data	
Ideal formula	Ag_4TeS
Crystal system	monoclinic
Space group	$P2_1/n$
Unit-cell parameters (Å, °)	4.2696(4) 6.9761(5) 8.0423(7) 90.00 100.332(6) 90.00
Unit-cell volume (Å^3)	235.66(3)
Z	4
Crystal size (mm)	0.060×0.055×0.040
Data collection	
Diffractometer	Oxford Xcalibur 3
Temperature (K)	293(2)
Radiation, wavelength (Å)	Mo*K*α 0.71073
2θ max for data collection (º)	69.96
Crystal-detector dist. (mm)	50
h, *k*, *l* ranges	-6 – 6, -11 – 11, -12 – 12
Axis, frames, width (º), time per frame (s)	ω/φ, 1211, 1.00, 70
Total reflections collected	3911
Unique reflections (R_{int})	956 (0.041)
Unique reflections $I > 2\sigma(I)$	418
Data completeness to θ_{max} (%)	99.6
Absorption correction method	ABSPACK (Oxford Diffraction 2006)
Structure refinement	
Refinement method	Full-matrix least-squares on F^2
Data/restraints/parameters	956/0/29
R_1 [$I > 2\sigma(I)$], wR_2 [$I > 2\sigma(I)$]	0.0298, 0.0560
R_1 all, wR_2 all	0.0329, 0.0562
Goodness-of-fit on F^2	0.975
Largest diff. peak and hole (e$^-$/Å^3)	0.76, -0.45

$$R_{int} = (n/n-1)^{1/2}\left[F_o^{\,2} - F_o(mean)^2\right]/\sum F_o^2$$

$$R_1 = \sum \| F_o| - |F_c \| / \sum |F_o| \qquad wR_2 = \left\{\sum\left[w\left(F_o^2 - F_c^2\right)^2\right]/\sum\left[w\left(F_o^2\right)^2\right]\right\}^{1/2}$$

$$GooF = \left\{\sum\left[w\left(F_o^2 - F_c^2\right)^2\right]/(n-p)\right\}^{1/2}$$ where n = no. of reflections, p = no. of refined parameters

Table
Click here to download Table: Bindi et al_Table 2.doc

TABLE 2 – Atoms, Wyckoff letter, site occupancy, fractional atom coordinates (Å), and isotropic atomic displacement parameters (Å^2) for cervelleite

atom	Wyckoff	site occupancy	*x*	*y*	*z*	U_{eq}
Ag1	4*e*	$Ag_{1.00}$	0.7542(3)	0.0339(1)	0.34094(8)	0.0244(2)
Ag2	4*e*	$Ag_{1.00}$	0.2887(2)	0.3487(1)	0.41168(8)	0.0261(2)
X	4*e*	$Te_{0.527(3)}S_{0.473}$	0.3608(2)	0.2417(2)	0.13068(9)	0.0296(3)

Table
Click here to download Table: Bindi et al_Table 3.doc

TABLE 3 – Selected bond distances (Å) for cervelleite

Ag1	- X	2.600(1)	Ag2	- X	2.451(1)	Ag1	-Ag2 3.041(1)
	- X	2.603(1)		- X	2.815(1)		-Ag2 3.079(1)
	- X	2.776(1)		- X	2.821(1)		-Ag2 3.083(1)
<Ag1-X>		2.660		- X	2.827(1)		-Ag2 3.145(1)
			<Ag2-X>		2.729		-Ag2 3.321(1)
						Ag2	-Ag2 2.968(1)

Table
Click here to download Table: Bindi et al_Table 4.doc

TABLE 4 – Calculated powder diffraction pattern for cervelleite

h	*k*	*l*	I_{calc}	*d*(Å)
1	1	1	21	3.1009
-1	1	2	100	2.8923
1	2	0	61	2.6834
-1	2	1	43	2.6347
0	2	2	8	2.6163
1	1	2	56	2.4791
0	1	3	23	2.4669
1	2	1	71	2.4571
-1	0	3	33	2.4392
0	3	1	39	2.2310
0	2	3	13	2.1037
2	0	0	37	2.1002
1	0	3	6	2.0724
-1	3	1	6	2.0129
2	1	0	19	2.0110
0	3	2	36	2.0047
-1	2	3	19	1.9989
1	1	3	17	1.9866
0	0	4	29	1.9780
-2	1	2	10	1.9317
0	3	3	9	1.7442
-2	2	2	12	1.7417
0	4	1	7	1.7031
-1	2	4	8	1.6872
-1	4	1	8	1.6000
-2	0	4	11	1.5892
-2	3	1	7	1.5693
-2	3	2	6	1.5208
2	3	1	11	1.4920
-1	3	4	9	1.4841
2	1	3	7	1.4812
-1	2	5	5	1.4370
-2	3	3	8	1.4276
-3	1	2	8	1.3739
1	3	4	8	1.3603
-2	4	1	6	1.3486
-1	5	1	12	1.3181
3	1	1	7	1.3142
2	1	4	7	1.3028
1	2	5	7	1.2995
1	5	1	7	1.2941
2	4	2	7	1.2285
-2	2	6	7	1.1513
-3	4	1	7	1.1026

d values calculated on the basis of a = 4.2694(4), b = 6.9761(5), c = 8.0423(7) Å, β = 100.332(6)°, and with the atomic coordinates and occupancies reported in Table 2.

Intensities calculated using XPOW software version 2.0 (Downs et al. 1993). Only $I > 5\sigma(I)$ are reported.

Table
Click here to download Table: Bindi et al_Table 5.doc

TABLE 5 – X-ray powder diffraction patterns for the unnamed Ag_2FeS_2 phase intergrown with cervelleite

	1			2		
hkl	d_{obs} (Å)	I_{obs}		I_{obs}	d_{obs} (Å)	I_{obs}
020	6.28	60		012	6.29	s
001	5.75	10		112	5.74	w
-101	5.00	100		022	5.00	vvs
-111	4.643	35		122,003	4.64	m
021	4.240	80		113	4.24	vs
121	3.761	35		123	3.766	ms
201	3.425	5		014,223	3.421	vw
230	3.061	5		–	–	–
-231	2.755	2		134,015	2.753	vw
311	2.529	5		n.i.	2.530	vw
212	2.308	10		016	2.304	w
-401	2.140	5		335	2.137	vw
-251	2.071	5		–	–	–
251	2.026	5		444	2.026	vw
061	1.9670	10		117,155	1.9659	vw
350	1.9242	5		146,027	1.9247	vw
-261	1.8170	5		n.i.	1.8174	vw

Note: 1 = observed powder pattern of the unnamed Ag_2FeS_2 phase of this study. 2 = observed powder pattern and indexing originally reported by Criddle et al. (1989) for 'cervelleite'.

Colour Figure
Click here to download high resolution image

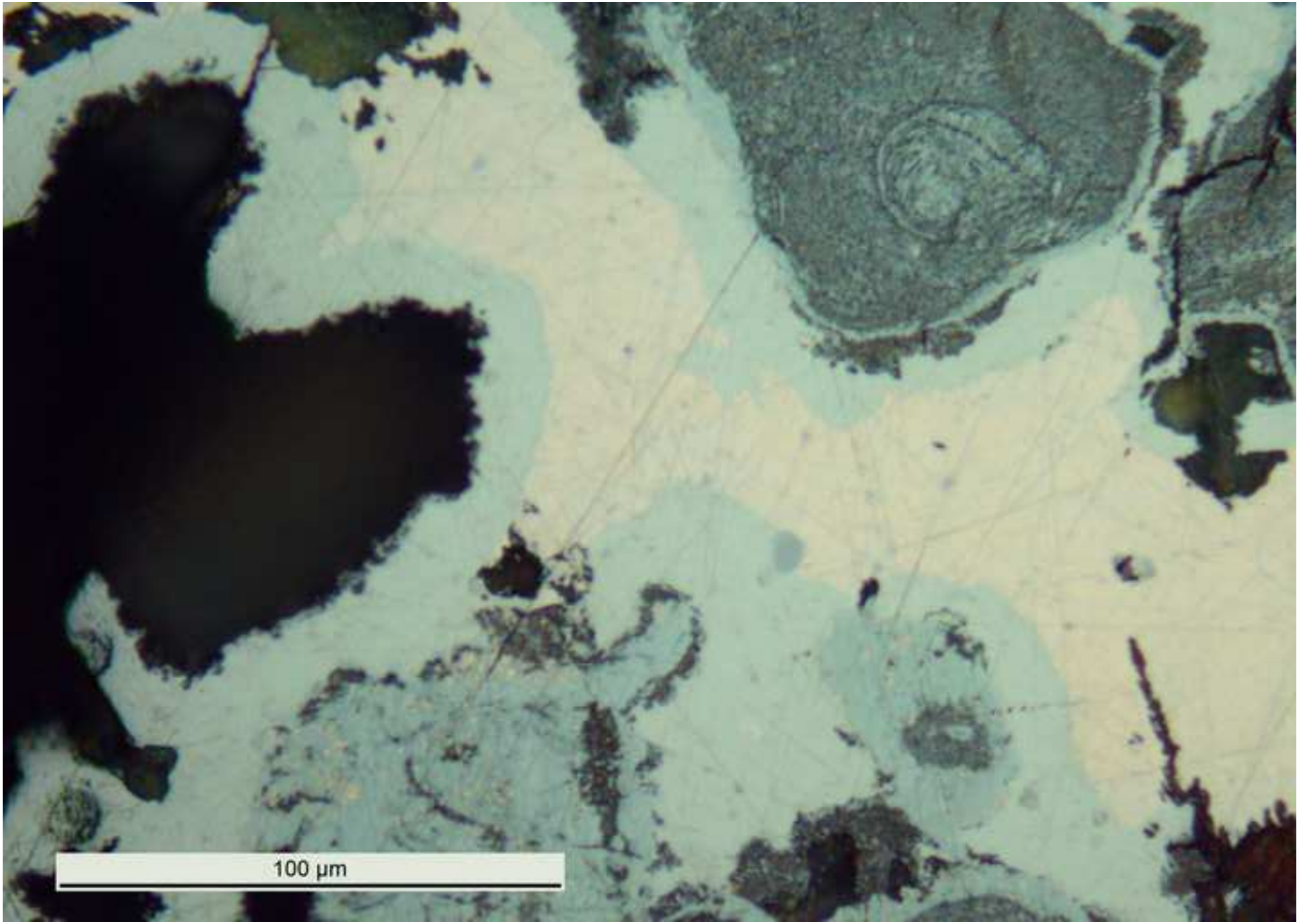

Line Figure
Click here to download high resolution image

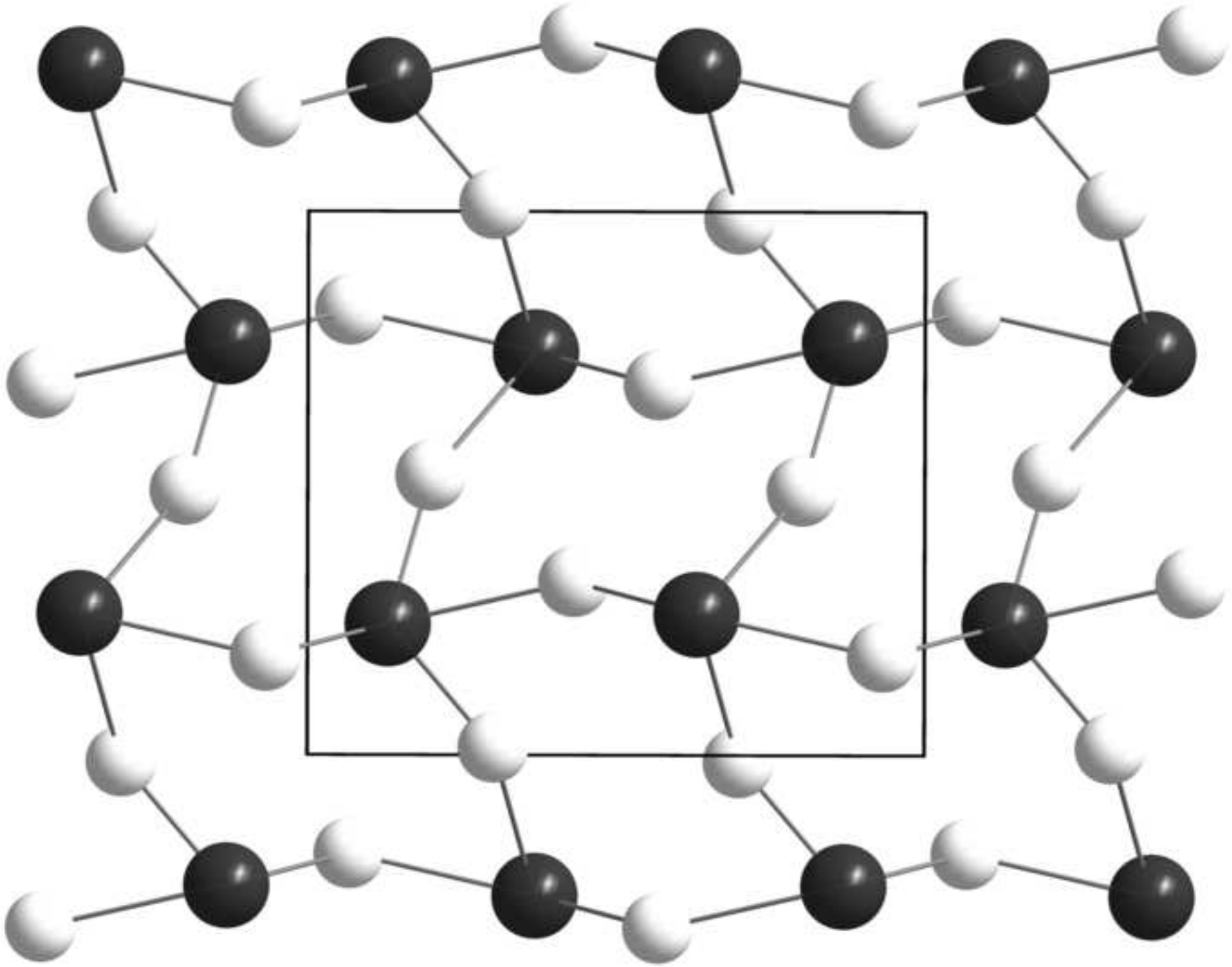

Line Figure
Click here to download high resolution image

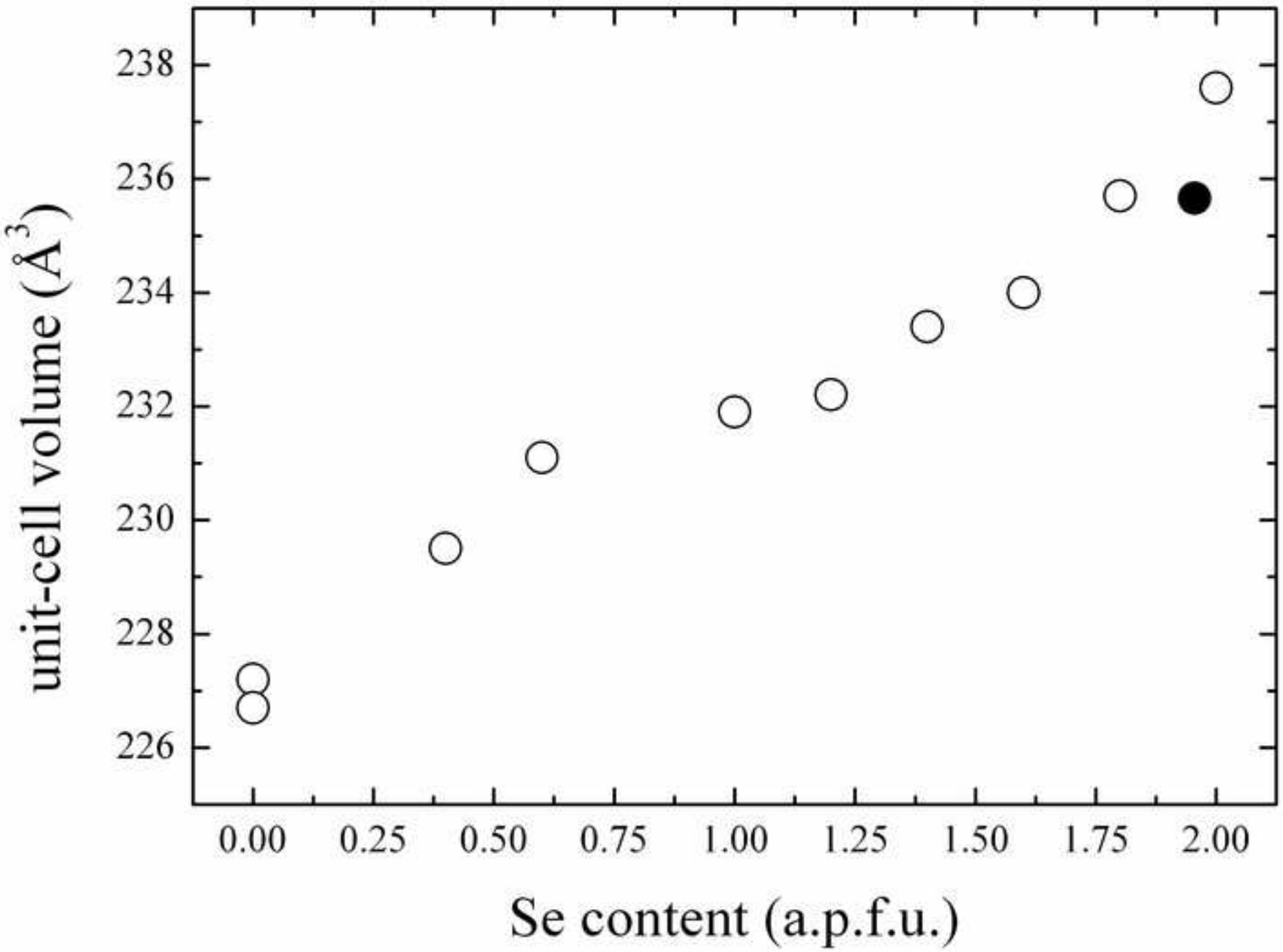

Line Figure
Click here to download high resolution image